Proceedings of the ASME 2011 Dynamic Systems and Control Conference
DSCC2011
October 31 - November 2, 2011, Arlington, VA, USA

DSCC2011-6193

STATE OF CHARGE ESTIMATION ERROR DUE TO PARAMETER MISMATCH IN A GENERALIZED EXPLICIT LITHIUM ION BATTERY MODEL

Xinfan Lin *
Anna Stefanopoulou
Department of Mechanical Engineering
University of Michigan
Ann Arbor, Michigan 48109
Email: xflin@umich.edu

Patricia Laskowsky
Jim Freudenberg
Department of Electrical Engineering
and Computer Science
University of Michigan
Ann Arbor, Michigan 48109

Yonghua Li
R. Dyche Anderson
Advanced Battery Controls
Research and Advanced Engineering
Ford Motor Company
Dearborn, Michigan 48124

ABSTRACT

Model-based state of charge (SOC) estimation with output feedback of the voltage error is steadily augmenting more traditional coulomb counting or voltage inversion techniques in hybrid electric vehicle applications. In this paper, the state (SOC) estimation error in the presence of model parameter mismatch is calculated for a general lithium ion battery model with linear diffusion or impedance-based state dynamics and nonlinear output voltage equations. The estimation error due to initial conditions and inputs is derived for linearized battery models and also verified by nonlinear simulations. It is shown that in some cases of parameter mismatch, the state, e.g. SOC, estimation error will be significant while the voltage estimation error is negligible.

1 INTRODUCTION

With a battery model available, it is a common practice to design an estimator with voltage feedback, such as a Luenberger observer or a Kalman filter, to estimate the internal states and then obtain the battery State of Charge (SOC), State of Power (SOP) and State of Health (SOH) [1–4]. According to linear system theory, if a plant model is observable and known perfectly, then one can design a stable observer so that the estimated states $\hat{x}$ and output $\hat{y}$ will converge to those of the real plant despite errors in initial conditions. In this way, an estimator with output feedback can be used to estimate the unmeasurable variables based on measurable ones, which cannot be achieved as well by open loop model when subject to unknown initial conditions, unmeasured disturbances and noise. For battery management applications, a Kalman filter is often applied to estimate *SOC* [1–3].

In applications, models may have different parameters from the real battery, referred to as parameter mismatch, for many reasons, such as cell to cell variation, temperature change, cell degradation and imprecise model identification. Many seminal papers have shown that adaptive schemes can be used to identify model parameters and then estimate the battery states [2, 4–7]. However, adaptive schemes and the parameter update law rely on the error between the predicted and the measured voltage, not the state (e.g. *SOC*), which can be more meaningful and critical. So it is of great practical interest to investigate the estimation errors in the presence of parameter mismatch, especially the errors in the state when the errors in voltage are negligible.

This work can be viewed as a precursor to a more formal and rigorous identifiability study similar to the one in [8]. The work in [8] utilized an implicit model of the electrolyte and solid diffusion coupled with a distributed current density. Important parameters were indicated by input (current)-output (voltage) relation but with limited information or insight on their importance and effect. This paper, instead, will focus on exploring the effects of inaccurate parameters on state estimation based on simpler models with voltage feedback. The asymptotic state error induced by parameter mismatch is calculated for linearized battery models, and simulated for nonlinear models with voltage feedback. This work can guide adaptive schemes in selecting the critical set of parameters or strengthen modeling efforts by pointing to the important features to be captured in a control-oriented model.

In Section 2, a generalized battery model formulation for simplified explicit electrode-averaged electrochemical models and equivalent circuit models is developed. Analytical derivations of state estimation error are performed in Section 3 for linearized battery models. Simulation results with nonlinear lithium

*Address all correspondence to this author.

ion battery models are used in Section 4 to further clarify the expected errors under model mismatches.

2 LITHIUM ION BATTERY MODEL

In this section, it is shown that many battery models can be generalized in a state-space representation with linear state equations, where the state matrix A depends on the diffusion-related dynamics, B on the capacity, and a nonlinear output equation for the voltage:

$$\dot{x} = Ax + Bu, \quad y = f(x,u). \tag{1}$$

The models considered are (i) a simplified electrochemical model describing the lithium ion transport during charging and discharging processes, (ii) equivalent circuit models, and in the simplest case, (iii) an OCV-R model using coulomb counting for SOC estimation.

An equivalent circuit model [9], as shown in Fig. 1, can be summarized with the state space representation

$$\frac{d}{dt}\begin{bmatrix} SOC \\ V_{c1} \\ \cdots \\ V_{cn} \end{bmatrix} = \begin{bmatrix} 0 & 0 & \cdots \\ 0 & \frac{-1}{R_{c1}C_1} & \cdots \\ & \cdots & \\ 0 & \cdots & \frac{-1}{R_{cn}C_n} \end{bmatrix} \begin{bmatrix} SOC \\ V_{c1} \\ \cdots \\ V_{cn} \end{bmatrix} + \begin{bmatrix} -\frac{1}{Q} \\ \frac{1}{C_1} \\ \cdots \\ \frac{1}{C_n} \end{bmatrix} I$$
$$V = OCV(SOC) - \sum_{i=1}^{n} V_{ci} - RI. \tag{2}$$

In Eq. (2), the first state captures the bulk charge (SOC). The resulting open circuit voltage (OCV) is connected in series with n R-C circuits, where the states are the capacitor voltages, V_{ci}. Using as input u the current I, which is positive for discharging, and output y as the terminal voltage V, the equivalent circuit model is clearly in the form of Eq. (1), where A is a diagonal matrix whose diagonal elements include the bulk SOC integrator and the negative inverse of all $R_{ci}C_i$ elements. B depends on the bulk capacity of the battery Q and the various capacitances C_i, and the output terminal voltage is the summation of OCV as a nonlinear function of SOC, the voltage across the capacitors V_{ci}, and voltage drop due to overpotential. Overpotential is here considered to be purely resistive, computed as the product of an internal resistance R and current I. It is noted that the OCV and all the resistances are potentially functions of temperature and SOC. Such variability and other uncertain factors, motivate this study on the effects of parameter mismatch on the SOC estimation error.

For simplicity, an OCV-R model will be used for analysis, shown in the dashed box in Fig. 1, which can be written:

$$\dot{SOC} = -\frac{I}{Q}, \quad V = OCV(SOC) - RI \tag{3}$$

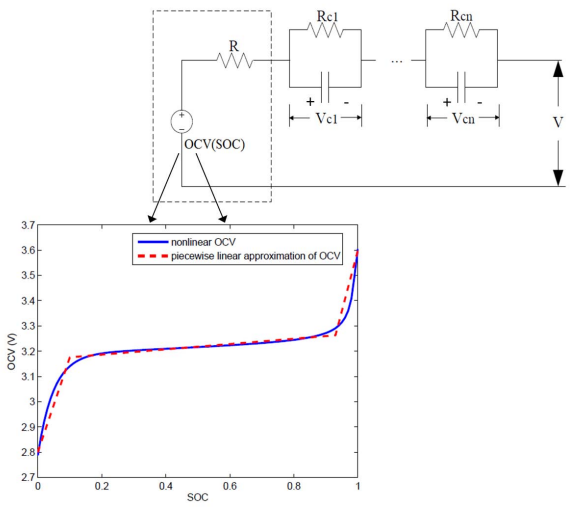

Figure 1. EQUIVALENT CIRCUIT MODEL SCHEMATIC [9]

where the state is SOC and the current I and voltage V correspond to input u and output y respectively. For the parameters, A is zero in this case, B is the inverse of the battery capacity Q, f is the nonlinear OCV function, and R is the internal resistance.

Eq. (1) can also be used for a control-oriented simplified electrochemical model [1], as shown in Fig. 2. In this model,

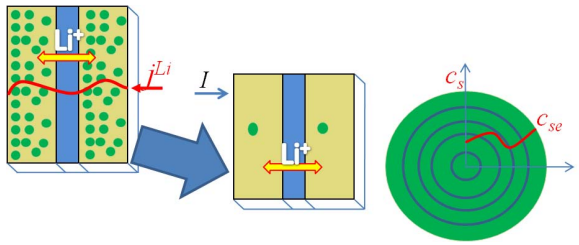

Figure 2. SIMPLIFIED ELECTROCHEMICAL MODEL SCHEMATIC [1]

lithium ions migrate between cathode and anode spherical representative particles during the charging and discharging processes. The lithium storage medium, the cathode particle here, is sliced into n pieces, and the concentration of each slice c_{si} constitutes one state. The SOC is related to the bulk lithium concentration, which is calculated as the average of all the states. The input is the external current I addressing the galvanostatic operation, and the output is the terminal voltage V. The model can be written as

$$\frac{d}{dt}\begin{bmatrix} c_{s1} \\ c_{s2} \\ \cdots \\ c_{sn} \end{bmatrix} = \frac{D_s}{\Delta_r^2}\begin{bmatrix} -2 & 2 & 0 & \cdots \\ \frac{1}{2} & -2 & \frac{3}{2} & \cdots \\ 0 & 0 & \ddots & 0 \\ 0 & \cdots & \frac{n-1}{n} & -\frac{n-1}{n} \end{bmatrix} \begin{bmatrix} c_{s1} \\ c_{s2} \\ \cdots \\ c_{sn} \end{bmatrix} + \frac{1}{A_e \delta F a_s \Delta_r} \begin{bmatrix} 0 \\ 0 \\ \cdots \\ \frac{n+1}{n} \end{bmatrix} I$$
$$V = OP(c_{sn}, I) + OCV(c_{sn}) - R_f I. \tag{4}$$

The state matrix A is now the diffusion dynamic matrix, basically the discrete implementation of Fick's 2nd law. Input matrix B is related to the electrode dimensions relevant to capacity. Specifically, A_e is the electrode area, δ is the electrode thickness, a_s is active particle surface and Δr is the spatial discretization parameter. The concentration at the particle-electrolyte interface, c_{se}, is related to the last state c_{sn} and represents the lithium immediately available. It can be viewed as the *SOP* [5]. The terminal voltage V consists of the overpotential OP as a nonlinear function of c_{se} and current, OCV, and a lumped ohmic voltage drop.

Based on the analysis of the above three very common models, the state(s) x for a lithium ion battery model is the energy storage level, either lithium concentrations or *SOC*, input u is current I, and the output y is the terminal voltage V, which is described by a nonlinear function f of the state and input.

A typical OCV profile of a $LiFePO_4/C$ battery is shown in Fig. 1. Such a nonlinear OCV function is flat in the middle *SOC* range and quite steep at the two ends, and thus it can be approximated by a piecewise linear function with three pieces as shown in Fig. 1. More complicated nonlinear OCV profiles can be linearized around multiple nominal points, and such piecewise linear representations are very convenient for control analysis and design. The states, input and output of the model are now the deviation of variables around nominal points. The previous nonlinear OCV function is replaced by linearized approximations.

Specifically, after linearization, the nonlinear OCV function for an OCV-R model becomes

$$\delta V = \alpha \delta SOC - R\delta I \tag{5}$$

where $\alpha = \frac{\partial OCV}{\partial SOC}\big|_{SOC_0}$ is the slope of the OCV curve at a nominal point SOC_0. The voltage function for the equivalent circuit model in Eq. (2) will turn into

$$\delta V = \alpha \delta SOC - R_1 \delta I - \sum_{i=1}^{n} \delta V_{ci}. \tag{6}$$

The voltage function for the simplified electrochemical model in Eq. (4) will now be

$$\delta V = \begin{bmatrix} 0 \cdots & \frac{\partial OP}{\partial c_{sn}} + \frac{\partial OCV}{\partial c_{sn}} \end{bmatrix} \begin{bmatrix} \delta c_{s1} \\ \cdots \\ \delta c_{sn} \end{bmatrix} + \left(\frac{\partial OP}{\partial I} - R_f \right) \delta I. \tag{7}$$

In summary, Eq. (1) fits some of the most commonly used control-oriented battery models in galvanostatic mode with voltage feedback. The state matrix A represents model dynamics, the input matrix B is capacity dependent, the voltage approximated by $y = Cx + Du$, where C depends on the slope of the OCV curve, and D directly corresponds to the lumped ohmic resistance. This way, the model formulation in Eq. (1) can be used as a general form in the subsequent analysis. It is also interesting to note that there is always one and only one eigenvalue at zero for those lithium ion battery models considered, which captures the accumulation of Li concentration or bulk *SOC*. In this paper, we are concerned with bounded input, bounded output stability, and thus the eigenvalue at zero, which represents an integrator, is unstable. Dynamics associated with stable poles will diminish in steady state while those associated with unstable poles will remain and might even grow unbounded. The unstable eigenvalue of the battery model is an important physical attribute and will be explored in the subsequent derivations of *SOC* estimation error.

3 ESTIMATION ERROR ANALYSIS FOR GENERAL LINEAR BATTERY MODELS

An observer for linear systems takes the form

$$\dot{\hat{x}} = A\hat{x} + Bu + L(y - \hat{y}), \quad \hat{y} = C\hat{x} + Du \tag{8}$$

where $\hat{x}$ and $\hat{y}$ are estimated states and output and L is the observer gain. The difference between the measured and the estimated output is used as feedback to correct the estimated states. For an actual lithium ion battery, there could be parameter mismatch due to cell to cell variation, temperature change and cell degradation, so it is of practical interest to quantify those estimation errors and evaluate which modeling error is the most critical to reduce during the modeling phase or with on-line adaptation.

In this section, estimation errors will be defined first and their response to inputs and initial conditions will be derived for a general linearized battery model. Detailed analysis of model errors for the linear model will then be performed based on the error transfer functions.

3.1 Derivation for Estimation Errors

If the model parameters are not known perfectly for the observer, the whole system takes the form

$$\begin{aligned} &\dot{x} = Ax + Bu, \quad y = Cx + Du \\ &\dot{\hat{x}} = \hat{A}\hat{x} + \hat{B}u + L(y - \hat{y}), \quad \hat{y} = \hat{C}\hat{x} + \hat{D}u \\ &x \in \mathbb{R}^n \quad u \in \mathbb{R}^1 \quad y \in \mathbb{R}^1 \end{aligned} \tag{9}$$

where $\hat{A}$, $\hat{B}$, $\hat{C}$, and $\hat{D}$ represent the parameters adopted for the observer, which might be different from the real parameters A, B, C and D. Note here that x_0 and $\hat{x}_0$ is the deviation of states from the nominal point. For general battery models, there could be more than one state, such as spatially varying concentrations for electrochemical models, but one output (voltage). Denote the state and output estimation errors by

$$e_x = x - \hat{x}, \quad e_y = y - \hat{y}. \tag{10}$$

The Laplace transforms of e_x and e_y are given by

$$\begin{aligned} E_x(s) =& (sI-\hat{A}+L\hat{C})^{-1}\big([e_{x,0}+(\Delta A-L\Delta C)(sI-A)^{-1}x_0] \\ &+[(\Delta A-L\Delta C)(sI-A)^{-1}B+\Delta B-L\Delta D]U(s)\big) \\ E_y(s) =& \frac{C(sI-A)^{-1}x_0-\hat{C}(sI-\hat{A})^{-1}\hat{x}_0}{[1+\hat{C}(sI-\hat{A})^{-1}L]} \\ &+\frac{C(sI-A)^{-1}B-\hat{C}(sI-\hat{A})^{-1}\hat{B}+\Delta D}{1+\hat{C}(sI-\hat{A})^{-1}L}U(s) \end{aligned} \tag{11}$$

where $e_{x,0}=x_0-\hat{x}_0\neq 0$, $\Delta A=A-\hat{A}$, $\Delta B=B-\hat{B}$, $\Delta C=C-\hat{C}$, and $\Delta D=D-\hat{D}$ denote the mismatch between modeled and real parameters. The impact of the initial conditions and inputs on the estimation errors will be evaluated in the subsequent sections.

3.2 Analysis of the Estimation Error due to unknown initial conditions

In this section we consider only the response to initial conditions and thus assume that the current input is equal to zero. It follows from Eq. (11) that

$$E_y(s)=\frac{C(sI-A)^{-1}x_0}{1+\hat{C}(sI-\hat{A})^{-1}L}-\frac{\hat{C}(sI-\hat{A})^{-1}\hat{x}_0}{1+\hat{C}(sI-\hat{A})^{-1}L}. \tag{12}$$

It can be shown by the following analysis that the steady state errors for e_y will be zero if the unstable dynamics of the real battery are accurately modeled in the observer. The unstable dynamics consists of the single eigenvalue at the origin, representing the bulk *SOC* state, and it is reasonable to assume that the observer also contains an integrator to model the accumulation/depletion of the lithium ion. Hence the voltage estimation error will be asymptotically equal to zero, even under parameter mismatch. Eq. (12) is now used to derive this conclusion.

By applying the easily proven matrix identity $(I+\hat{C}(sI-\hat{A})^{-1}L)^{-1}\hat{C}(sI-\hat{A})^{-1}=\hat{C}(sI-\hat{A}+L\hat{C})^{-1}$, we have that the second term on the right hand side of Eq. (12), which is the error induced by $\hat{x}_0$, is equal to $\hat{C}(sI-\hat{A}+L\hat{C})^{-1}\hat{x}_0$. Its poles are the eigenvalues of the observer, denoted as λ_{CLE}. As long as the estimator is designed to be asymptotically stable, λ_{CLE} will be stable and converge to zero eventually.

The first term on the right hand side of Eq. (12), which is the error induced by x_0, is denoted as

$$\begin{aligned} &\frac{C(sI-A)^{-1}x_0}{1+\hat{C}(sI-\hat{A})^{-1}L}=\frac{\hat{D}(s)}{D(s)}\frac{N(s)}{\hat{D}(s)+\hat{N}(s)} \\ &C(sI-A)^{-1}x_0=\frac{N(s)}{D(s)},\quad 1+\hat{C}(sI-\hat{A})^{-1}L=1+\frac{\hat{N}(s)}{\hat{D}(s)}. \end{aligned} \tag{13}$$

It is clear that the roots of $D(s)$ are the eigenvalues of A, denoted as λ_A, the roots of $\hat{D}(s)$ are the eigenvalues of $\hat{A}$, denoted as $\lambda_{\hat{A}}$, and the roots of $\hat{D}(s)+\hat{N}(s)$ are the eigenvalues of the observer, λ_{CLE}. It can be argued that if $\hat{A}$ has the unstable eigenvalue of A at zero, i.e. the model captures the bulk charge integrator, the unstable roots of $D(s)$ and $\hat{D}(s)$ will get canceled in Eq. (13). Hence the poles for the first term on the right hand side of Eq. (12) will be the stable roots of $\hat{D}(s)+\hat{N}(s)$, λ_{CLE}, and the uncanceled stable eigenvalues of A. In this way, the steady state value for the first term on the right hand side of Eq. (12) will be zero.

Based on the above analysis, when $\hat{A}$ models the bulk charge integrator, $E_y(s)$ can be written by partial fraction expansion as

$$E_y(s)=\left(\sum_{i=1}^{n}\frac{R_{CLE,i}^{x_0\to y}}{s-\lambda_{CLE,i}}+\sum_{i=1}^{k}\frac{R_{A\neq\hat{A},i}^{x_0\to y}}{s-\lambda_{A\neq\hat{A},i}}\right)x_0+\sum_{i=1}^{n}\frac{R_{CLE,i}^{\hat{x}_0\to y}}{s-\lambda_{CLE,i}}\hat{x}_0 \tag{14}$$

where $R_{CLE,i}^{x_0\to y}$ are the residues of the error induced by x_0 associated with λ_{CLE}, $R_{A\neq\hat{A},i}^{x_0\to y}$ are residues of the error induced by x_0 associated with eigenvalues of A that are not canceled by $\hat{A}$, namely $\lambda_{A\neq\hat{A},i}$, and $R_{CLE,i}^{\hat{x}_0\to y}$ are the residues of the error induced by $\hat{x}_0$ associated with the eigenvalues of the observer. The steady state value of e_y will be zero since all the poles are stable.

An OCV-R model can be used for illustration, where $A=\hat{A}=0$, and Eq. (14) becomes

$$E_V(s)=\frac{\alpha\delta SOC_0-\hat{\alpha}\delta S\hat{O}C_0}{s+\hat{\alpha}L}, \tag{15}$$

where δSOC_0 and $\delta S\hat{O}C_0$ are the deviation of the battery and estimator *SOC* from the nominal point. The steady state error will be zero.

A similar analysis can be conducted for e_x. If only the unforced response of the state estimation error is considered, $E_x(s)$ can be reduced to

$$E_x(s)=(sI-\hat{A}+L\hat{C})^{-1}[e_{x,0}+(\Delta A-L\Delta C)(sI-A)^{-1}x_0]. \tag{16}$$

It can be observed that the poles of E_x are the eigenvalues of the observer, λ_{CLE}, and the eigenvalues of A, λ_A. The unstable pole of A might result in a non-zero steady state e_x. Partial fraction expansion for Eq. (16) shows

$$E_x(s)=\sum_{i=1}^{n}\frac{R_{CLE,i}^{e_{x,0}\to x}}{s-\lambda_{CLE,i}}e_{x,0}+\sum_{i=1}^{n}\left(\frac{R_{CLE,i}^{x,0\to x}}{s-\lambda_{CLE,i}}+\frac{R_{A,i}^{x_0\to x}}{s-\lambda_{A,i}}\right)x_0 \tag{17}$$

where $R_{CLE,i}^{e_{x,0}\to x}$ are the residues of $E_{x,e_{x0}}(s)$ associated with eigenvalue $\lambda_{CLE,i}$, $R_{CLE,i}^{x,0\to x}$ are the residues of $E_{x,x_0}(s)$ associated with eigenvalue $\lambda_{CLE,i}$ and $R_{A,i}^{x_0\to x}$ are the residues of $E_{x,x_0}(s)$ associated with the eigenvalue of A matrix $\lambda_{A,i}$. The term $\frac{R_{A,0}^{x_0\to x}}{s}x_0$ associated with $\lambda_{A,0}=0$ of A contributes a steady state error.

Taking an OCV-R model for illustration, Eq. (17) becomes

$$E_{SOC}(s) = \frac{se_{SOC,0} - L\Delta\alpha\delta SOC_0}{s(s+L\hat{\alpha})} \tag{18}$$

with steady state error

$$e_{SOC}(\infty) = -\frac{\Delta\alpha}{\hat{\alpha}}\delta SOC_0, \tag{19}$$

which indicates that the final error in *SOC* estimation due to initial errors is proportional to the mismatch in OCV slope $\Delta\alpha$ and the deviation of the initial battery from the nominal point δSOC_0.

3.3 Analysis of Estimation Error Response to Input

This section evaluates the estimator errors in the presence of parameter mismatch when current is applied to the battery. When only the input is considered, E_x and E_y are obtained by keeping the second term on the right hand side of Eq. (11) as

$$\begin{aligned} E_x(s) =& (sI - \hat{A} + L\hat{C})^{-1}[(\Delta A - L\Delta C)(sI - A)^{-1}B \\ &+ \Delta B - L\Delta D]U(s) \\ E_y(s) =& \frac{C(sI-A)^{-1}B - \hat{C}(sI-\hat{A})^{-1}\hat{B} + \Delta D}{1 + \hat{C}(sI-\hat{A})^{-1}L}U(s) \end{aligned} \tag{20}$$

As to be expected, the estimation errors during charging and discharging will be affected not only by the mismatch in system dynamics ($\hat{A} \neq A$) and OCV ($\hat{C} \neq C$), but also by the mismatch in capacity ($\hat{B} \neq B$) and resistance ($\hat{D} \neq D$).

3.3.1 Estimation Errors induced by Mismatch in Capacity (ΔB).

If only mismatch in capacity (ΔB) is considered, it is going to be shown that the estimation errors for both the states and the output will be finite when subject to bounded inputs. In this case, Eq. (20) can be reduced to

$$\begin{aligned} E_x(s) &= (sI - A + LC)^{-1}\Delta BU(s) \\ E_y(s) &= \frac{C(sI-A)^{-1}\Delta B}{1 + C(sI-A)^{-1}L}U(s). \end{aligned} \tag{21}$$

The poles of $E_x(s)$ will be the eigenvalues of the observer, λ_{CLE}, which are all stable. $E_y(s)$ can be proven to be equal to $C(sI - A + LC)^{-1}\Delta BU(s)$, and then it is obvious that

$$E_x(s) = \sum_{i=1}^{n} \frac{R^{u\to x}_{CLE,i}}{s - \lambda_{CL,i}}U(s), \quad E_y(s) = \sum_{i=1}^{n} \frac{R^{u\to y}_{CLE,i}}{s - \lambda_{CL,i}}U(s). \tag{22}$$

The poles of both E_x and E_y will be the λ_{CLE}. Since all the poles of the observer, λ_{CLE}, are stable, the error response to step input will be finite in steady state.

If an OCV-R model is used as an example, Eq. (22) becomes

$$E_{SOC}(s) = \frac{\Delta Q}{Q\hat{Q}(s+L\alpha)}I(s), \quad E_V(s) = \frac{\alpha\Delta Q}{Q\hat{Q}(s+L\alpha)}I(s) \tag{23}$$

and their steady state values will be

$$e_{SOC}(\infty) = \frac{\Delta Q}{Q\hat{Q}L\alpha}I, \quad e_V(\infty) = \frac{\Delta Q}{Q\hat{Q}L}I. \tag{24}$$

From Eq. (24) it can be seen that mismatch in capacity (ΔQ) will result in finite errors for both *SOC* and voltage estimation when subject to fixed current input. The errors are proportional to the amount of mismatch and the current magnitude. Increasing the observer gain L amplifies such errors but makes estimation more sensitive to measurement noise.

3.3.2 Estimation Errors induced by Mismatch in OCV Slope (ΔC).

When there is only mismatch in the local slope of the OCV curve (C), it can be established that the steady state error in output estimation, E_y, will be finite while the error in state estimation will be an integral of current over time. Under this scenario, $E_x(s)$ and $E_y(s)$ can be obtained as

$$\begin{aligned} E_x(s) &= -(sI - A + L\hat{C})^{-1}L\Delta C(sI-A)^{-1}BU(s) \\ E_y(s) &= \frac{\Delta C(sI-A)^{-1}B}{1 + \hat{C}(sI-A)^{-1}L}U(s). \end{aligned} \tag{25}$$

For $E_y(s)$, by following the same argument as in Eq. (13), it can be established that all its poles are the eigenvalues of the observer, which are all stable and thus e_y will converge to a finite steady state error.

For $E_x(s)$, its poles consist of the eigenvalues of the observer and the A matrix. Thus the transfer functions will have one unstable pole corresponding to the zero eigenvalue of A. Hence the *SOC* estimation error will be an integral of the current over time. The significance of this error depends on the practical operation in most applications, where the current is cut off when the battery hits a certain voltage limit. In this way, this error will stop growing and be bounded by the operating range of the battery.

For an OCV-R model, $E_{SOC}(s)$ and $E_V(s)$ will be

$$E_{SOC} = \frac{-\Delta\alpha}{Q\hat{\alpha}}\left(\frac{1}{s} - \frac{1}{s+L\hat{\alpha}}\right)I(s), E_V = \frac{\Delta\alpha}{Q(s+L\hat{\alpha})}I(s). \tag{26}$$

As shown in Eq. (26), the estimation errors for *SOC* will be an integral of current over time due to a pole at zero. The estimation error for voltage will reach $\frac{\Delta\alpha}{Q\hat{\alpha}L}I$, which is proportional to the amount of mismatch in the local OCV slope. Increasing L reduces the error in voltage estimation.

3.3.3 Estimation Errors induced by Mismatch in Resistance (ΔD).

In this case, e_x will converge to a finite value when subject to step inputs, while e_y will be zero in steady state. These facts follow by simplifying Eq. (20):

$$\begin{aligned} E_x(s) &= -(sI - A + LC)^{-1} L\Delta D U(s) \\ E_y(s) &= \frac{\Delta D}{1 + C(sI - A)^{-1} L} U(s). \end{aligned} \tag{27}$$

The poles of both $E_x(s)$ and $E_y(s)$ are the eigenvalues of the closed loop observer, indicating finite steady state estimation errors. Furthermore, it can be proven that $E_y(s)$ has zero at the origin which is the eigenvalue of A. Consequently, the steady state error for output estimation subject to step inputs will be zero.

The OCV-R model can also be used as an example for illustration, where

$$E_{SOC}(s) = -\frac{L\Delta R}{s + L\alpha} I(s), \quad E_V(s) = \frac{\Delta R s}{s + L\alpha} I(s) \tag{28}$$

and the steady state values will be

$$e_{SOC}(\infty) = \frac{\Delta R}{\alpha} I, \quad , e_V(\infty) = 0. \tag{29}$$

3.3.4 Estimation Errors induced by Mismatch in System Dynamics (ΔA).

The forced responses of the estimation errors when there is only mismatch in system dynamics A are given by

$$\begin{aligned} E_x(s) &= (sI - \hat{A} + LC)^{-1} \Delta A (sI - A)^{-1} B U(s) \\ E_y(s) &= \frac{C(sI - A)^{-1} B - C(sI - \hat{A})^{-1} B}{1 + C(sI - \hat{A})^{-1} L} U(s). \end{aligned} \tag{30}$$

As for the mismatch in system dynamics ΔA, the only unstable eigenvalue for the general battery models considered in Section 2 is the one at zero. The dynamic matrix $\hat{A}$ of the observer is most likely going to preserve that zero eigenvalue since it predicts the bulk *SOC* behavior. Consequently, ΔA, if any, will be caused by a mismatch of the stable eigenvalues of the A matrix and the resultant steady state errors will be finite. Quantitative analysis of the effect of ΔA will have to deal with the specific structure of a battery model, and is now under investigation for the general battery models discussed earlier.

To summarize the results of Section 3.3, the estimation errors induced by current inputs are different in the presence of different parameter mismatch. A mismatch in capacity (B) will induce finite steady state errors in both voltage estimation and *SOC* estimation. A mismatch in local OCV slope (C) may cause finite steady state errors in voltage estimation while the errors in *SOC* estimation will be an integral of current over time, due to an unstable pole at zero in its transfer function. If there is mismatch in resistance (D), voltage estimation will not be affected under step inputs but a finite *SOC* estimation error will be induced at steady state. The steady state errors due to mismatches in capacity and local OCV slope can be reduced by increasing the observer gain L at the cost of sensitivity to measurement noise.

4 SIMULATION FOR NONLINEAR MODELS WITH EXTENDED KALMAN FILTER

Simulation of nonlinear lithium ion battery models is conducted to augment the theoretical conclusions for linearized cases. Specifically, an extended Kalman filter is applied for state estimation, where the nonlinear function mapping the state to the output is preserved,

$$\begin{aligned} \dot{x} &= Ax + Bu, \quad y = f(x,u) \\ \dot{\hat{x}} &= \hat{A}\hat{x} + \hat{B}u + L(y - \hat{y}), \quad \hat{y} = \hat{f}(\hat{x},u). \end{aligned} \tag{31}$$

The observer gain L is tuned based on model fidelity and measurement noise. With an extended Kalman filter, there would be no approximation errors brought by linearization and the analysis can be extended to the whole range of operation instead of a certain region around nominal point. An OCV-R model is used here for simulation with constant charging current applied. The OCV curve of a 55mAh A123 $LiFePO_4$ pouch cell taken from experiment is used here for simulation. The OCV and mismatched OCV curves are shown in Fig. 3. Simulation results are shown

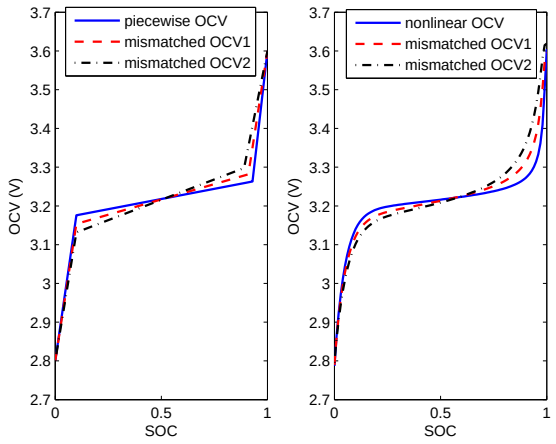

Figure 3. OCV MISMATCHES.

in Fig. 4, Fig. 5, Fig. 6 and Fig. 7.

Estimation errors due to initial conditions are simulated by using the nonlinear OCV and mismatched OCV curves shown at the right side of Fig. 3, where there is a larger mismatch in OCV2

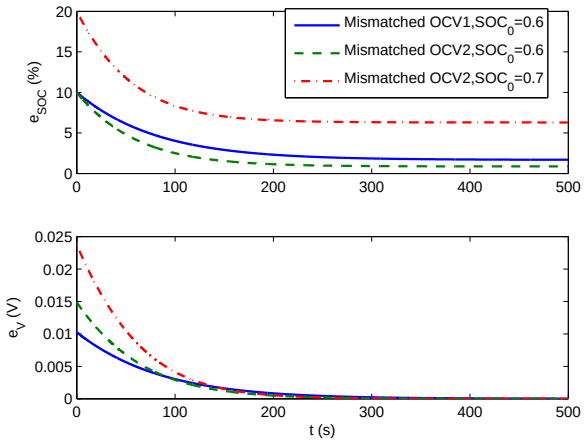

Figure 4. ERRORS FOR SOC AND VOLTAGE ESTIMATION SUBJECT TO INITIAL CONDITIONS.

than in OCV1. It is shown in Fig. 4 that errors in voltage estimation always go to zero. But the steady state *SOC* estimation error depends on the extent of mismatch in OCV and the initial *SOC* deviation from the 50% point, where the OCV curve and the mismatched ones are pinned. These are in accordance with the conclusions from the linear derivation in Eq. (19).

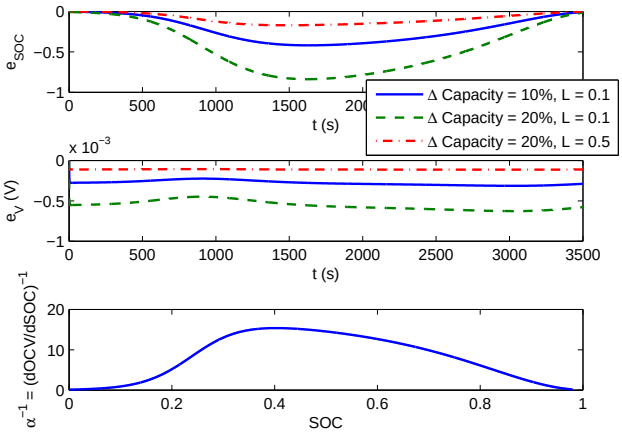

Figure 5. ERRORS FOR SOC AND VOLTAGE ESTIMATION INDUCED BY MISMATCH IN CAPACITY SUBJECT TO FIXED CURRENT INPUT.

When there is only mismatch in capacity (B), the battery model is simulated by charging from 0% to 100% *SOC*, and thus the time scale $0-3500s$ for the estimation errors corresponds to 0% to 100% *SOC* in a linear relation in Fig. 5. Since the OCV-R model has no extra dynamics besides an integrator and the error dynamics for the observer are fast, e_{SOC} and e_V can be viewed as in quasi steady state in Fig. 5. It can be seen that both estimation errors are proportional to the amount of mismatch in capacity and the inverse of L. As obtained in Eq. (24), the steady state e_{SOC} is proportional to α^{-1}, which is the inverse of the slope of the OCV curve, and thus it follows the shape of α^{-1} from 0% to 100% *SOC*, as shown in Fig. 5. Consequently, the maximum error occurs in the flat middle *SOC* range, where α^{-1} reaches maximum. Meanwhile, e_V will be more consistent because its steady state value obtained from linear derivation is not related to α according to Eq. (24) and its values are quite small.

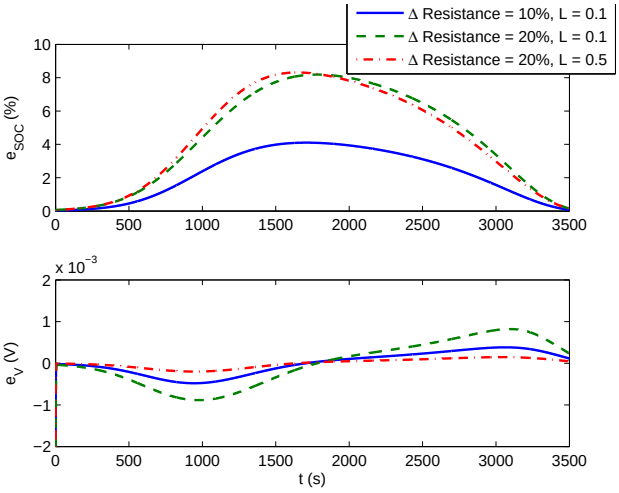

Figure 6. ERRORS FOR SOC AND VOLTAGE ESTIMATION INDUCED BY MISMATCH IN RESISTANCE SUBJECT TO CURRENT INPUT.

For mismatch in resistance D, the battery is also simulated by charging from 0% to 100% *SOC*. The *SOC* estimation error is proportional to the amount of mismatch (ΔD), and the voltage estimation error fluctuates around zero, as shown in Fig. 6. Observer gain L doesn't have much effect here. Similar to the case of mismatch in capacity (B), as predicted by Eq. (29), e_{SOC} follows the shape of α^{-1} from 0% to 100% *SOC*, and the maximum error occurs in the flat middle *SOC* range as α^{-1} reaches its peak. Linear derivation also supports the nonlinear simulation where the steady state e_V fluctuates around zero.

For mismatch in the OCV curve, simulations have been conducted with both nonlinear OCV functions and piecewise linear approximations. It is noted that due to the flatness of the OCV curve in the middle *SOC* range, small measurement errors in the intermediate points, e.g. 10-20mV, which are quite typical in industrial applications, can result in significant mismatch in the slope of the OCV curve in that range, as shown in Fig. 3. Step current input simulation starts at 50%*SOC* to give zero initial estimation error. As predicted by Eq. (26), simulation with the piecewise linear approximation of OCV in Fig. 3 shows that e_{SOC} response is an integral of current over time in the middle piece of the OCV curve, and simulation with nonlinear OCV curves demonstrates similar growing e_{SOC}. The growing rate of such errors are determined by the extent of mismatch and smaller L will slow down error dynamics, which are also in accordance with Eq. (26). When *SOC* goes beyond the flat middle range, e_{SOC}

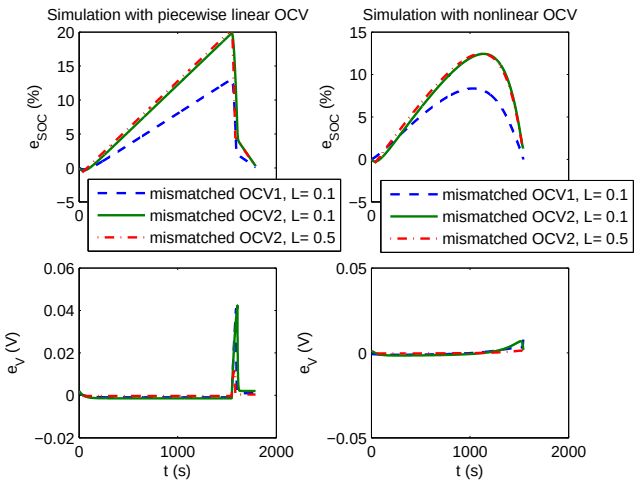

Figure 7. ERRORS FOR SOC AND VOLTAGE ESTIMATION INDUCED BY MISMATCH IN OPEN CIRCUIT VOLTAGE CURVE SLOPE SUBJECT TO FIXED CURRENT INPUT.

drops back to zero because the mismatched curves are pinned at the end. The error e_V is generally negligible comparing to e_{SOC}.

5 CONCLUSION

In this paper, voltage and SOC estimation errors in the presence of battery model parameter mismatch are investigated. A summary of the calculations is listed in Tab. (1). It is clear that model parameter mismatches can cause significant state (*SOC*) estimation error while the voltage estimation error is generally negligible. Therefore, although an estimator with voltage feedback can significantly reduce the errors in voltage estimation in the presence of parameter mismatches, it is still highly desirable to obtain accurate model parameters for precise *SOC* estimation.

The OCV curve may have a major impact on the estimation error behavior. It can be quite flat and close to linear in the middle *SOC* range, and thus mismatch in the slope of OCV curve can be easily created by small measurement errors. This will cause the *SOC* estimation error to grow as an integral of current over time in the middle *SOC* range. For hybrid electric vehicles, it can be problematic since they usually operate in that range and the e_{SOC} at the two ends of that range can be significant. For battery electric vehicles, although the error in *SOC* estimation is small near 0% and 100%, the erroneous estimation of *SOC* in the middle range might cause some gauge problems for the customers, e.g. over or under-estimation of the navigation range. In addition, the flatness of the OCV curve in the middle *SOC* range will also amplify the *SOC* estimation errors caused by mismatch in other battery parameters. Clearly, efforts to tailor lithium ion battery chemistry to avoid the flat OCV regions will help in *SOC* estimation [10]. Until then, OCV parameterization and its change during battery aging needs carefully modeling and characterization even with the most advanced *SOC* estimation algorithms.

Table 1. ESTIMATION ERRORS IN THE PRESENCE OF PARAMETER MISMATCH SUBJECT TO INITIAL CONDITIONS AND INPUTS.

	e_{SOC}	e_V
SOC_0,$\hat{SOC}_0$	$\propto (\Delta C, SOC_0)$	0
$I, \Delta B(Capacity)$	$\propto (\Delta B, \frac{1}{L}, \alpha^{-1})$	$\propto (\Delta B, \frac{1}{L})$
$I, \Delta C(OCV)$	$\propto (\int Idt, \Delta\alpha)$	$\propto (\Delta C, \frac{1}{L})$
$I, \Delta D(Resistance)$	$\propto \Delta D, \alpha^{-1}$	0

REFERENCES

[1] Domenico, D. D., Stefanopoulou, A., and Fiengo, G., 2010. "Lithium-ion battery state of charge and critical surface charge estimation using an electrochemical model-based extended kalman filter". *Journal of Dynamic Systems, Measurement, and Control,* **132**, p. 061302 (11 pages).

[2] Barbarisi, O., Vasca, F., and Glielmo, L., 2006. "State of charge kalman filter estimator for automotive batteries". *Control Engineering Practice,* **14**(3), pp. 267–275.

[3] Santhanagopalan, S., and White, R. E., 2006. "Online estimation of the state of charge of a lithium ion cell". *Journal of Power Sources,* **16**(2), pp. 1346–1355.

[4] Plett, G. L., 2004. "Extended kalman filtering for battery management systems of lipb-based hev battery packs part 3. state and parameter estimation". *Journal of Power Sources,* **134**, p. 277C292.

[5] Verbrugge, M., and Tate, E., 2004. "Adaptive state of charge algorithm for nickel metal hydride batteries including hysteresis phenomena". *Journal of Power Sources,* **126**(1-2), pp. 236–249.

[6] Lee, S., Kim, J., Lee, J., and Cho, B., 2008. "State-of-charge and capacity estimation of lithium-ion battery using a new open-circuit voltage versus state-of-charge". *Journal of Power Sources,* **185**(2), pp. 1367–1373.

[7] Pop, V., Bergveld, H., Danilov, D., Notten, P., and Regtien, P., 2007. "Adaptive state-of-charge indication system for li-ion battery-powered devices". *The World Electric Vehicle Association Journal,* **1**, pp. 38–45.

[8] Schmidt, A. P., Bitzer, M., and Guzzella, L., 2010. "Experiment-driven electrochemical modeling and systematic parameterization for a lithium-ion battery cell". *Journal of Power Sources,* **195**, pp. 5071–5080.

[9] Hu, Y., Yurkovich, S., Guezennec, Y., and Yurkovich, B., 2010. "Electro-thermal battery model identification for automotive applications". *Journal of Power Sources,* **196**, pp. 449–457.

[10] Wang, J., Verbrugge, M. W., and Liu, P., 2010. "Composite titanatecgraphite negative electrode for improved state-of-charge estimation of lithium-ion batteries". *Journal of The Electrochemical Society,* **157**, pp. A185–A189.